remote sensing

MDPI

Supplementary Materials:

Supplementary Materials: Monitoring Surface Deformation Over a Failing Rock Slope with the ESA Sentinels: Insights from Moosfluh Instability, Swiss Alps

Andrea Manconi [1,*], Penelope Kourkouli [1,2], Rafael Caduff [2], Tazio Strozzi [2] and Simon Loew [1]

[1] Department of Earth Sciences, Engineering Geology, Swiss Federal Institute of Technology, ETH Zurich, Sonneggstrasse 5, 8092 Zurich, Switzerland; penelope.kourkouli@erdw.ethz.ch (P.K.); simon.loew@erdw.ethz.ch (S.L.)

[2] Gamma Remote Sensing AG, Worbstrasse 225, 3073 Gümligen, Switzerland; caduff@gamma-rs.ch (R.C.); strozzi@gamma-rs.ch (T.S.)

Table S1. Sentinel-1 dataset. List of images used in this study. Track 066, Descending orbit. Data retrieved from Copernicus Open Access Hub (https://scihub.copernicus.eu/).

Scene identifier
S1A_IW_SLC__1SDV_20170304T053456_20170304T053523_015538_01988A_5A26.zip
S1B_IW_SLC__1SDV_20170310T053359_20170310T053426_004642_008186_5B01.zip
S1B_IW_SLC__1SDV_20170310T053424_20170310T053451_004642_008186_B695.zip
S1A_IW_SLC__1SDV_20170316T053457_20170316T053524_015713_019DC6_BB3D.zip
S1A_IW_SLC__1SDV_20170328T053457_20170328T053524_015888_01A304_E8A4.zip
S1B_IW_SLC__1SDV_20170403T053425_20170403T053451_004992_008BB2_3052.zip
S1B_IW_SLC__1SDV_20170403T053400_20170403T053427_004992_008BB2_66B3.zip
S1A_IW_SLC__1SDV_20170409T053457_20170409T053524_016063_01A842_FEE6.zip
S1B_IW_SLC__1SDV_20170415T053400_20170415T053427_005167_0090B0_18F0.zip
S1B_IW_SLC__1SDV_20170415T053425_20170415T053452_005167_0090B0_8BA2.zip
S1A_IW_SLC__1SDV_20170421T053458_20170421T053525_016238_01AD9E_C86F.zip
S1B_IW_SLC__1SDV_20170427T053425_20170427T053452_005342_0095D4_F5B7.zip
S1B_IW_SLC__1SDV_20170427T053401_20170427T053428_005342_0095D4_607D.zip
S1A_IW_SLC__1SDV_20170503T053459_20170503T053526_016413_01B2EC_8BE7.zip
S1A_IW_SLC__1SDV_20170515T053459_20170515T053526_016588_01B83E_6C94.zip
S1B_IW_SLC__1SDV_20170521T053407_20170521T053433_005692_009F8E_DAAC.zip
S1A_IW_SLC__1SDV_20170527T053451_20170527T053518_016763_01BD9F_5D86.zip
S1B_IW_SLC__1SDV_20170602T053432_20170602T053459_005867_00A499_656D.zip
S1B_IW_SLC__1SDV_20170602T053407_20170602T053434_005867_00A499_A351.zip
S1A_IW_SLC__1SDV_20170608T053441_20170608T053508_016938_01C30F_89BC.zip
S1A_IW_SLC__1SDV_20170608T053506_20170608T053533_016938_01C30F_659A.zip
S1B_IW_SLC__1SDV_20170614T053408_20170614T053435_006042_00A9BE_0B85.zip
S1B_IW_SLC__1SDV_20170614T053433_20170614T053500_006042_00A9BE_101C.zip
S1A_IW_SLC__1SDV_20170620T053442_20170620T053509_017113_01C876_B4CF.zip
S1A_IW_SLC__1SDV_20170620T053507_20170620T053534_017113_01C876_482D.zip
S1B_IW_SLC__1SDV_20170626T053409_20170626T053436_006217_00AED5_DE2C.zip
S1B_IW_SLC__1SDV_20170626T053433_20170626T053500_006217_00AED5_2174.zip
S1A_IW_SLC__1SDV_20170702T053507_20170702T053534_017288_01CDBA_B2C3.zip
S1A_IW_SLC__1SDV_20170702T053443_20170702T053510_017288_01CDBA_E982.zip
S1A_IW_SLC__1SDV_20170714T053443_20170714T053510_017463_01D304_CF30.zip
S1A_IW_SLC__1SDV_20170714T053508_20170714T053535_017463_01D304_3A60.zip

S1B_IW_SLC__1SDV_20170720T053410_20170720T053437_006567_00B8C9_6F04.zip
S1B_IW_SLC__1SDV_20170720T053435_20170720T053502_006567_00B8C9_417B.zip
S1A_IW_SLC__1SDV_20170807T053445_20170807T053512_017813_01DDB3_99FC.zip
S1A_IW_SLC__1SDV_20170807T053510_20170807T053537_017813_01DDB3_89F4.zip
S1B_IW_SLC__1SDV_20170813T053436_20170813T053503_006917_00C2E7_638B.zip
S1B_IW_SLC__1SDV_20170813T053411_20170813T053438_006917_00C2E7_8739.zip
S1A_IW_SLC__1SDV_20170819T053510_20170819T053537_017988_01E302_EF1A.zip
S1A_IW_SLC__1SDV_20170819T053445_20170819T053512_017988_01E302_6DE8.zip
S1B_IW_SLC__1SDV_20170825T053412_20170825T053439_007092_00C7F7_8018.zip
S1B_IW_SLC__1SDV_20170825T053437_20170825T053504_007092_00C7F7_27AF.zip
S1A_IW_SLC__1SDV_20170831T053511_20170831T053538_018163_01E845_CCA9.zip
S1A_IW_SLC__1SDV_20170831T053446_20170831T053513_018163_01E845_0E40.zip
S1B_IW_SLC__1SDV_20170906T053412_20170906T053439_007267_00CD0C_D6AE.zip
S1B_IW_SLC__1SDV_20170906T053437_20170906T053504_007267_00CD0C_A35A.zip
S1A_IW_SLC__1SDV_20170912T053511_20170912T053538_018338_01EDBF_14D0.zip
S1A_IW_SLC__1SDV_20170912T053446_20170912T053513_018338_01EDBF_823C.zip
S1B_IW_SLC__1SDV_20170918T053413_20170918T053440_007442_00D231_F6E1.zip
S1B_IW_SLC__1SDV_20170918T053438_20170918T053505_007442_00D231_B4E3.zip
S1A_IW_SLC__1SDV_20170924T053511_20170924T053538_018513_01F31D_26C4.zip
S1A_IW_SLC__1SDV_20170924T053447_20170924T053514_018513_01F31D_788D.zip
S1B_IW_SLC__1SDV_20170930T053413_20170930T053440_007617_00D737_2765.zip
S1B_IW_SLC__1SDV_20170930T053438_20170930T053505_007617_00D737_DFEE.zip
S1A_IW_SLC__1SDV_20171006T053512_20171006T053539_018688_01F871_B1C5.zip
S1A_IW_SLC__1SDV_20171006T053447_20171006T053514_018688_01F871_977D.zip
S1B_IW_SLC__1SDV_20171012T053413_20171012T053440_007792_00DC33_287C.zip
S1B_IW_SLC__1SDV_20171012T053438_20171012T053505_007792_00DC33_AC9E.zip
S1A_IW_SLC__1SDV_20171018T053447_20171018T053514_018863_01FDCC_C816.zip
S1A_IW_SLC__1SDV_20171018T053512_20171018T053539_018863_01FDCC_DC72.zip
S1B_IW_SLC__1SDV_20171024T053413_20171024T053440_007967_00E134_7376.zip
S1B_IW_SLC__1SDV_20171024T053438_20171024T053505_007967_00E134_71DE.zip
S1A_IW_SLC__1SDV_20171030T053447_20171030T053514_019038_02031F_A8FD.zip
S1A_IW_SLC__1SDV_20171030T053512_20171030T053539_019038_02031F_7C0A.zip

Table S2. Sentinel-2 dataset. List of images used in this study. Relative Orbits R065 and R108. Data retrieved from Copernicus Open Access Hub (https://scihub.copernicus.eu/).

Scene identifier
S2A_MSIL2A_20170420T103021_N0204_R108_T32TMS_20170420T103454.zip
S2A_MSIL2A_20170427T102031_N0205_R065_T32TMS_20170427T102025.zip
S2A_MSIL2A_20170430T103021_N0205_R108_T32TMS_20170430T103024.zip
S2A_MSIL2A_20170507T102031_N0205_R065_T32TMS_20170507T102319.zip
S2A_MSIL2A_20170510T103031_N0205_R108_T32TMS_20170510T103025.zip
S2A_MSIL2A_20170517T102031_N0205_R065_T32TMS_20170517T102352.zip
S2A_MSIL2A_20170527T102031_N0205_R065_T32TMS_20170527T102301.zip
S2A_MSIL2A_20170530T103021_N0205_R108_T32TMS_20170530T103024.zip
S2A_MSIL2A_20170606T102031_N0205_R065_T32TMS_20170606T102456.zip
S2A_MSIL2A_20170609T103021_N0205_R108_T32TMS_20170609T103023.zip
S2A_MSIL2A_20170616T102021_N0205_R065_T32TMS_20170616T102331.zip
S2A_MSIL2A_20170619T103021_N0205_R108_T32TMS_20170619T103021.zip
S2A_MSIL2A_20170626T102021_N0205_R065_T32TMS_20170626T102321.zip
S2A_MSIL2A_20170629T103021_N0205_R108_T32TMS_20170629T103020.zip
S2A_MSIL2A_20170706T102021_N0205_R065_T32TMS_20170706T102301.zip
S2A_MSIL2A_20170709T103021_N0205_R108_T32TMS_20170709T103159.zip
S2A_MSIL2A_20170719T103021_N0205_R108_T32TMS_20170719T103023.zip
S2A_MSIL2A_20170726T102021_N0205_R065_T32TMS_20170726T102259.zip
S2A_MSIL2A_20170805T102031_N0205_R065_T32TMS_20170805T102535.zip
S2A_MSIL2A_20170808T103021_N0205_R108_T32TMS_20170808T103023.zip
S2A_MSIL2A_20170815T102021_N0205_R065_T32TMS_20170815T102513.zip
S2A_MSIL2A_20170818T103021_N0205_R108_T32TMS_20170818T103421.zip
S2A_MSIL2A_20170825T102021_N0205_R065_T32TMS_20170825T102114.zip
S2A_MSIL2A_20170904T102021_N0205_R065_T32TMS_20170904T102511.zip
S2A_MSIL2A_20170907T103021_N0205_R108_T32TMS_20170907T103021.zip
S2A_MSIL2A_20170914T102021_N0205_R065_T32TMS_20170914T102559.zip
S2A_MSIL2A_20170917T103021_N0205_R108_T32TMS_20170917T103018.zip
S2A_MSIL2A_20170924T102021_N0205_R065_T32TMS_20170924T102649.zip
S2A_MSIL2A_20170927T103021_N0205_R108_T32TMS_20170927T103018.zip
S2A_MSIL2A_20171004T102021_N0205_R065_T32TMS_20171004T102021.zip
S2A_MSIL2A_20171007T103021_N0205_R108_T32TMS_20171007T103241.zip
S2A_MSIL2A_20171014T102021_N0205_R065_T32TMS_20171014T102235.zip
S2A_MSIL2A_20171017T103021_N0205_R108_T32TMS_20171017T103024.zip
S2A_MSIL2A_20171024T102111_N0206_R065_T32TMS_20171024T140204.zip
S2A_MSIL2A_20171027T103131_N0206_R108_T32TMS_20171027T141000.zip

Table S3. List of Sentinel-1 differential interferograms processed in this study, with indication of perpendicular (Bperp, im meters) and temporal baselines (Btemp, in days).

Image pair	Bperp (m)	Btemp (days)
20170304-20170310	131.13	5.99
20170304-20170316	116.41	12.00
20170310-20170316	-14.71	6.00
20170316-20170328	52.27	12.00
20170328-20170403	-120.23	5.99
20170328-20170409	-28.27	12.00
20170403-20170409	91.96	6.00
20170403-20170415	38.65	12.00
20170409-20170415	-53.31	5.99
20170409-20170421	-56.18	12.00
20170415-20170421	-2.86	6.00
20170415-20170427	69.05	12.00
20170421-20170427	71.92	5.99
20170421-20170503	26.64	12.00
20170427-20170503	-45.28	6.00
20170503-20170515	17.61	12.00
20170515-20170521	-2.10	5.99
20170515-20170527	-43.98	12.00
20170521-20170527	-41.88	6.00
20170521-20170602	-128.77	12.00
20170527-20170602	-86.88	5.99
20170527-20170608	91.06	12.00
20170602-20170608	177.95	6.00
20170602-20170614	101.87	12.00
20170608-20170614	-76.08	5.99
20170608-20170620	-61.67	12.00
20170614-20170620	14.40	6.00
20170614-20170626	9.00	12.00
20170620-20170626	-5.40	5.99
20170620-20170702	-60.38	12.00
20170626-20170702	-54.98	6.00
20170702-20170714	10.69	12.00
20170714-20170720	46.65	5.99
20170714-20170726	11.38	12.00
20170720-20170726	-35.26	6.00
20170720-20170801	-21.42	12.00
20170726-20170801	13.84	5.99
20170726-20170807	96.35	12.00
20170801-20170807	82.50	6.00
20170801-20170813	-37.01	12.00
20170807-20170813	-119.52	5.99
20170807-20170819	-78.19	12.00
20170813-20170819	41.32	6.00
20170813-20170825	61.97	12.00
20170819-20170825	20.64	5.99
20170819-20170831	-10.95	12.00
20170825-20170831	-31.60	6.00
20170825-20170906	-13.78	12.00
20170831-20170906	17.81	5.99

20170831-20170912	10.88	12.00
20170906-20170912	-6.93	6.00
20170906-20170918	69.76	12.00
20170912-20170918	76.69	5.99
20170912-20170924	4.27	12.00
20170918-20170924	-72.41	6.00
20170918-20170930	-65.85	12.00
20170924-20170930	6.55	5.99
20170924-20171006	42.28	12.00
20170930-20171006	35.73	6.00
20170930-20171012	-34.65	12.00
20171006-20171012	-70.38	5.99
20171006-20171018	-18.14	12.00
20171012-20171018	52.24	6.00
20171012-20171024	72.91	12.00
20171018-20171024	20.67	5.99
20171018-20171030	-5.05	12.00
20171024-20171030	-25.72	6.00

Table S4. Sentinel-2 dataset. Information on Moosfluh area visibility. About 60% of the available imagery was unusable for DIC due to local or regional cloud cover.

Date (yyyymmddThhmmss)	Orbit	Visibility (Y/N)
20170420T103021	R108	Y
20170427T102031	R065	N
20170430T103021	R108	Y
20170507T102031	R065	N
20170510T103031	R108	Y
20170517T102031	R065	Y
20170527T102031	R065	N
20170530T103021	R108	N
20170606T102031	R065	N
20170609T103021	R108	N
20170616T102021	R065	N
20170619T103021	R108	N
20170626T102021	R065	Y
20170629T103021	R108	N
20170706T102021	R065	Y
20170709T103021	R108	N
20170719T103021	R108	Y
20170726T102021	R065	N
20170805T102031	R065	Y
20170808T103021	R108	N
20170815T102021	R065	Y
20170818T103021	R108	N
20170825T102021	R065	Y
20170904T102021	R065	N
20170907T103021	R108	N
20170914T102021	R065	N
20170917T103021	R108	N
20170924T102021	R065	N
20170927T103021	R108	N
20171004T102021	R065	Y
20171007T103021	R108	Y
20171014T102021	R065	Y
20171017T103021	R108	Y
20171024T102111	R065	Y
20171027T103131	R108	N

Figure S1. Exemplary of pictures showing damage occurred at the Moosfluh slope after the summer 2016 crisis. Photos courtesy Franziska Glueer, ETH Zurich.

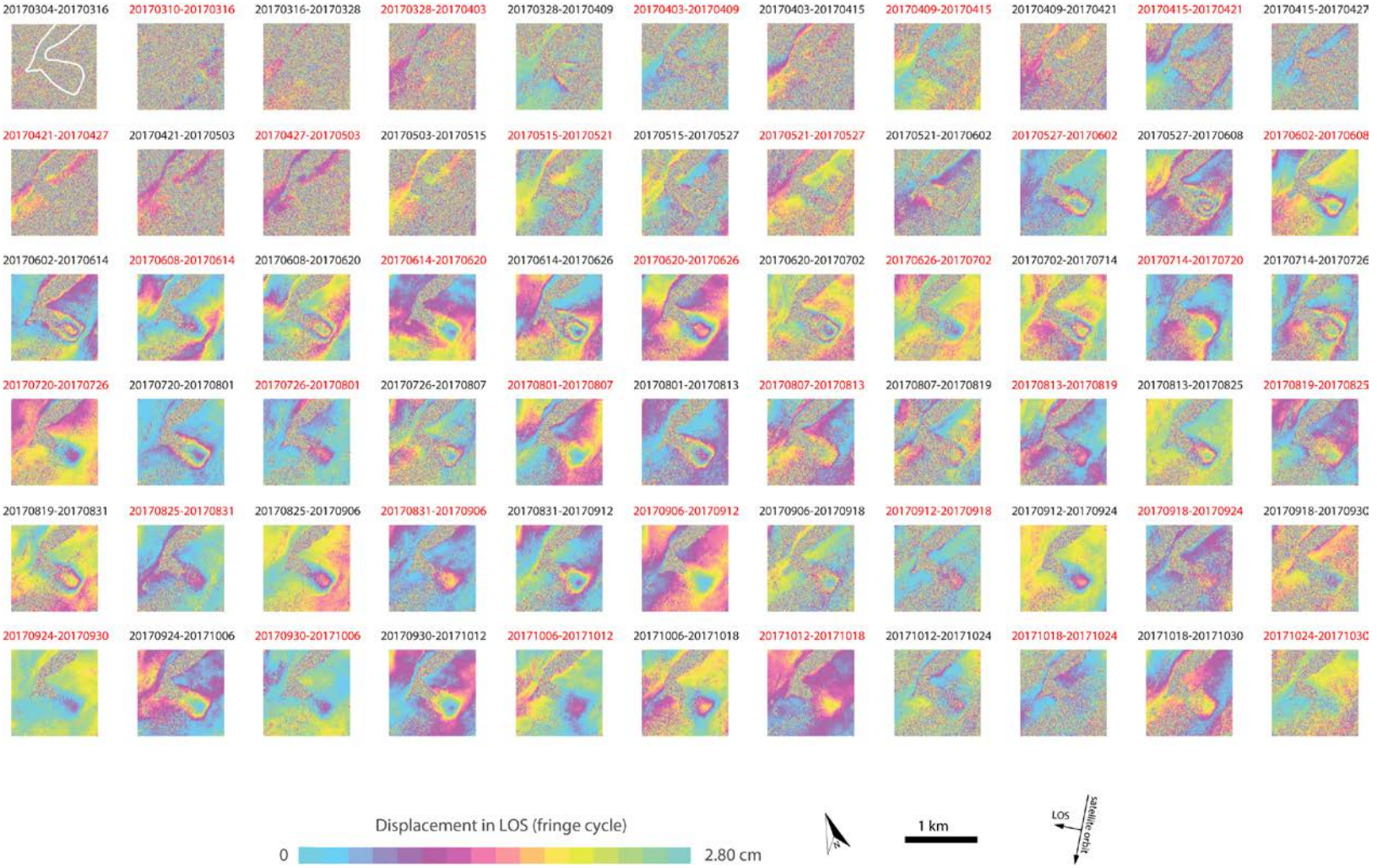

Figure S2. Full set of Sentinel-1 differential interferograms processed in this study. Time of acquisition for each SAR image pair analyzed is provided in the format YYYY.MM.DD (red=6-day separation, black= 12 days separation). White boundary in the upper left interferogram delineates the area of the Aletsch glacier and Moosfluh

slope instability (cf. Figure 1 in the main text). Differential interferograms were generated by using a high resolution DEM (SwissALTI3D, 2m GSD) and filtered [35] to increase signal-to-noise ratio.

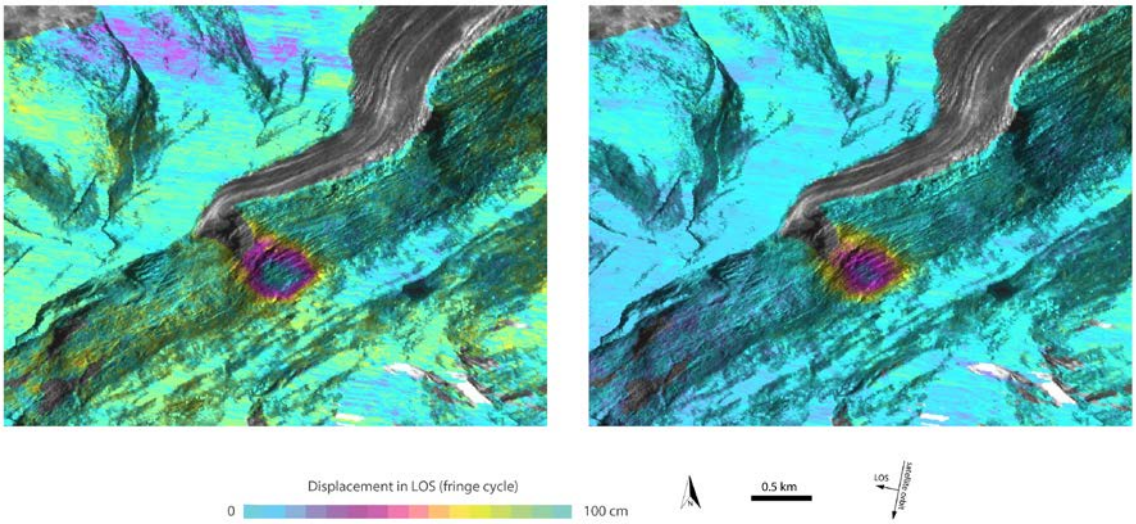

Figure S3. Stack of differential interferograms with 6-days (left) and 12-days (right) temporal separation. Areas with coherence lower than 0.4 are masked.

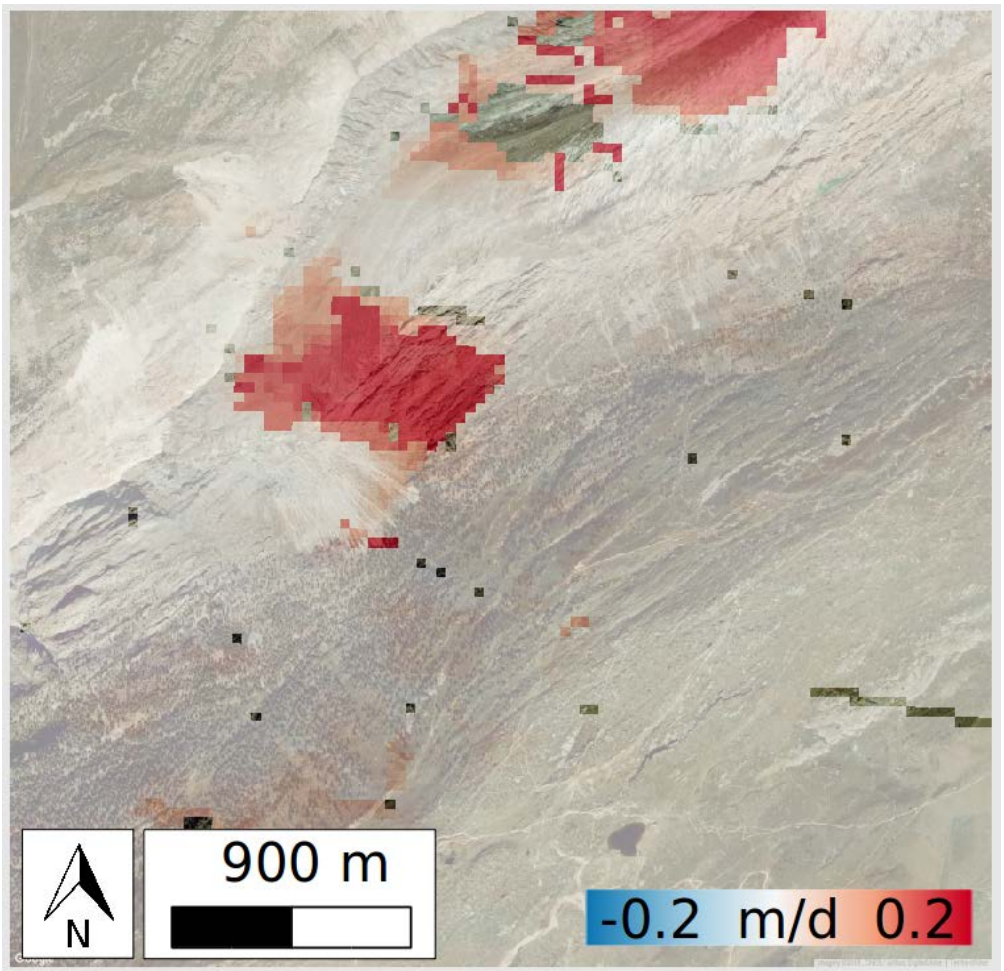

Figure S4. Digital Image Correlation results obtained with ALOS Palsar-2, by processing the pair of images acquired on August 8 and November 14, 2017. Despite increased GSD of the Palsar-2 sensor, accuracy of the DIC result is in the same range of what retrieved for Sentinel-1. Moreover, revisit time of Palsar-2 is too poor for monitoring purposes.